Calorimetric, spectroscopic, and structural studies of anhydrous zinc bromide

M. A. White, C. Chieh, A. Anderson, and L. A. K. Staveley

Calorimetric, spectroscopic, and structural studies of anhydrous zinc bromide

M. A. White[a] and C. Chieh

Guelph-Waterloo Centre for Graduate Work in Chemistry, Waterloo Campus, Waterloo, Ontario, N2L 3G1, Canada

A. Anderson

Guelph-Waterloo Program for Graduate Work in Physics, Waterloo Campus, Waterloo, Ontario, N2L 3G1, Canada

L. A. K. Staveley

Inorganic Chemistry Laboratory, University of Oxford, Oxford OX1 3QR, England

Measurements of the heat capacity of $ZnBr_2$ from $T = 10$ to 300 K, as well as Raman, infrared, and x-ray diffraction investigations reveal some very interesting features of this material. The unit cell (space group $I\,4_1/acd$) is large ($Z = 32$), and composed of supertetrahadral Zn_4Br_{10} subunits. The large unit cell and the large effective mass of the subunits, respectively, give rise to a rich vibrational spectrum and many low frequency modes. These have been used quantitatively to account for the unusually high heat capacity of $ZnBr_2$ at low temperatures.

INTRODUCTION

Interest in the magnetic phase transitions of $NiBr_2$,[1,2] as well as a theoretical prediction of the magnetic contribution to its heat capacity[3] recently prompted the first calorimetric investigation of $NiBr_2$.[4] In order to delineate the magnetic and lattice contributions to the heat capacity of $NiBr_2$, a measurement of the heat capacity of a supposedly isomorphous[5] diamagnetic compound of similar molecular weight, $ZnBr_2$, was undertaken. (The heat capacity of $ZnBr_2$ has not been reported previously.) However the heat capacity measurements indicated that $ZnBr_2$ could not have the $CdCl_2$ type structure that $NiBr_2$ has and that $ZnBr_2$ is often reported to have.[5,6] This conclusion prompted a complete x-ray diffraction study of $ZnBr_2$ which is reported in detail elsewhere.[7] The purpose of this communication is the presentation of the calorimetric results for $ZnBr_2$, as well as the results of Raman and infrared spectroscopic investigations and the correlation of these results with each other and with the x-ray diffraction information.

EXPERIMENTAL TECHNIQUES

Anhydrous zinc (II) bromide (Alpha Inorganics, 99% pure) was dried under vacuum at 200 °C for 6 h, and further purified by vacuum sublimation at 350 °C for 8 h. Sublimation produced a very fine powder which was then sealed under vacuum, heated to 410 °C (just above its melting point), and allowed to cool gradually to room temperature in order to produce small single crystals for the x-ray diffraction and larger crystallites for the Raman investigations. Chemical analysis gave the following results (theoretical mass % in brackets): Zn, 30.3 (29.0); Br, 71.1 (71.0). All sample handling was carried out in a dry nitrogen glove box because of the extreme hygroscopic nature of $ZnBr_2$.

The heat capacity of $ZnBr_2$ was measured from $T = 10$ K to $T = 300$ K by the heat pulse technique in an adiabatic calorimeter that was fitted with a calibrated Pt resistance thermometer. This calorimeter is described in detail elsewhere.[8]

X-ray diffraction data for a crystal of maximum and minimum dimensions 0.18 and 0.10 mm were collected on a Syntex $P\,2_1$ diffractometer. The crystal was sealed in a capillary tube, and 2988 reflections were collected.

Samples for the Raman experiments were crystallite fragments about $2 \times 2 \times 3$ mm. These were mounted on the cold finger of a standard glass cryostat and cooled by liquid nitrogen. Raman spectra were excited by the 514.5 nm line of an argon ion laser (Spectra Physics 165), operating at powers up to 1 W. Light scattered at 90° was focused on to the entrance slit of a double monochromator (Spex 1401). The polarization of the incident laser beam could be rotated by a Fresnel bi-prism, and the scattered light analyzed with a rotatable Polaroid film and quartz wedge ("scrambler") mounted in front of the entrance slit. For some experiments aimed at detecting weak features at very low frequencies a third monochromator (Spex 1442) was introduced into the light path. The detector was a cooled photomultiplier (R.C.A. C31024), coupled to photon counting electronics. Output pulses were fed to an IBM PC microcomputer for storage, display, plotting, and subsequent processing.

For the infrared experiments, polycrystalline fragments were ground to a fine powder by mortar and pestle inside a nitrogen-filled glove box. The powder was spread as evenly as possible on a polyethylene plate and then covered by a second plate. The "sandwich" was then clamped on to the cold finger of a glass crysostat, fitted with polyethylene windows. Temperatures for both Raman and infrared samples were measured by copper-Constantan thermocouples in pressure contact with the substrate. Far infrared spectra were recorded on a Beckman RIIC Fourier Spectrometer (F.S. 620) equipped with high pressure mercury lamp source, Mylar beam dividers, and germanium bolometric detector operating at 4.2 K. Fast Fourier transforms of the interfero-

---

[a] Present address: Chemistry Department, Dalhousie University, Halifax, Nova Scotia B3H 4J3, Canada.

TABLE I. Experimental values of the heat capacity (C_p) of ZnBr$_2$ from $T = 11$ to 300 K.

T (K)	C_p (J K^{-1} mol^{-1})	T (K)	C_p (J K^{-1} mol^{-1})	T (K)	C_p (J K^{-1} mol^{-1})
11.29	2.66	63.43	43.01	151.30	66.15
11.91	3.62	68.43	45.38	156.08	66.56
14.97	6.92	73.18	48.11	161.14	66.84
17.91	10.12	75.16	49.33	166.41	67.52
21.96	14.53	77.78	50.02	172.04	68.23
23.73	16.57	78.77	50.43	177.24	68.42
26.03	18.87	84.46	52.31	182.44	68.53
27.35	20.43	87.41	54.05	187.59	68.89
29.80	22.15	90.29	54.91	193.24	69.18
31.32	23.83	93.62	55.78	199.36	69.63
33.53	25.02	97.31	56.74	205.76	69.68
34.81	26.18	100.90	58.04	212.82	69.97
37.21	28.04	106.66	59.20	220.26	70.16
38.33	29.08	117.11	61.02	227.64	70.24
40.94	30.75	120.32	61.79	234.98	70.22
41.93	31.37	123.60	62.10	242.30	70.22
45.03	32.94	126.83	62.49	247.18	70.25
45.54	33.38	130.01	62.97	258.05	70.20
49.41	35.22	135.01	63.44	268.84	71.33
49.51	35.49	138.48	63.82	269.34	72.72
53.95	38.45	142.30	64.27	389.92	73.58
58.61	40.85	146.62	65.10	300.25	76.21

FIG. 2. Raman spectra of ZnBr$_2$ in comparison with that of NiBr$_2$. Lower curve is ZnBr$_2$ at $T = 125$ K, upper curve is ZnBr$_2$ at $T = 300$ K, and inset is NiBr$_2$ at $T = 110$ K for the same frequency range 25–205 cm^{-1}. NiBr$_2$ data from Ref. 13. Resolution: 1 cm^{-1}.

gram signals were performed by an IBM PC microcomputer, and sample spectra were ratioed against those from background runs.

RESULTS

The experimental values of the molar heat capacity of a finely powdered sample ($m = 23.491$ g) of ZnBr$_2$ are given in Table I and illustrated in Fig. 1. The sample comprised ~60% of the total heat capacity at $T = 10$ K, and decreased to ~40% of the total at $T = 300$ K. While no sample history effects were observed, the thermal relaxation time after the heat pulse was extraordinarily long in ZnBr$_2$. For example, at $T \sim 100$ K it was of the order of 1 h in the finely powdered sample, whereas other inorganic materials of similar sample morphology (such as NiBr$_2$) had given relaxation times of ~10 min in the same calorimeter. This observation, and the verification that the small amount ($\sim 10^{-1}$ Torr) of ^{3}He ex-

change gas in the sealed vessel had not escaped, led to an investigation of the heat capacity of a sample of ZnBr$_2$ that had been pelleted and then crushed to give pieces of the order of 1 mm in each dimension. This procedure was found to increase the relaxation time to several hours, and measurements on this second sample were therefore too inaccurate to be meaningful. (It is interesting to note that very long thermal relaxation times were also noticed in the measurement of the low temperature heat capacity of ZnCl$_2$[9] and PbI$_2$.[10] In the latter, the long relaxation has been ascribed to intrinsically low thermal conductivity of the sample. This is likely also the case in ZnBr$_2$.) However, the measured heat capacity of the finely powdered sample of ZnBr$_2$ (Fig. 1 and Table I) is not at all in doubt within an estimated error of $\pm 2\%$.

Raman spectra of anhydrous ZnBr$_2$ at 300 and 125 K are shown in Fig. 2, and peak frequencies at these two temperatures are listed in Table II. The usual sharpening of peaks and shifts to slightly higher frequencies as the lattice contracts on cooling are clearly seen. More unusual, however, are the changes in intensity observed, particularly for the triplet centered around 50 cm^{-1}. At first sight, this could be interpreted as evidence for a solid state phase transition, but the smooth heat capacity curve shows that this is not the case. Further study indicated that the phenomenon was related to polarization effects in the sample. Although single crystals large enough for Raman work could not be obtained, the samples used, probably consisting of conglomerates of a small number of single crystallites, did show polarization effects at room temperature. For some orientation combinations of polarizer and analyzer, changes in relative intensity similar to those seen in Fig. 3 were observed. In fact, we have used these properties to categorize many of the stronger peaks into the groups listed in Table II, following procedures used earlier for the alkali cyanides.[11] When the cryostat temperature was lowered, however, cracks and strains in the crystals resulted in multiple scattering and a complete and irreversible loss of polarization dependence. The observed changes in spectra at the two temperatures therefore reflect changes in the physical state of the sample (especially crystallite size and preferred or random orienta-
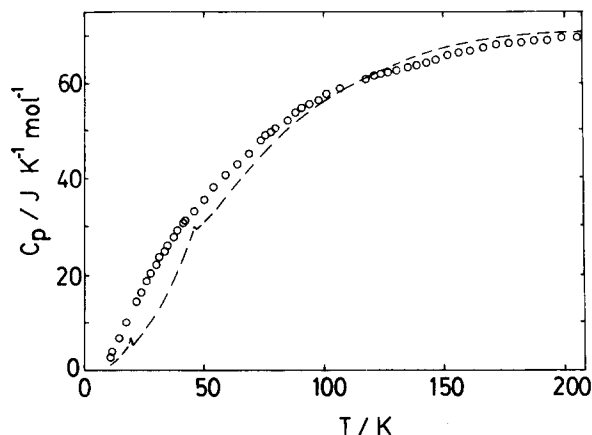

FIG. 1. The heat capacity of ZnBr$_2$ (open circles) as a function of temperatures, in comparison with that of NiBr$_2$ (dashed line). NiBr$_2$ data from Ref. 4.
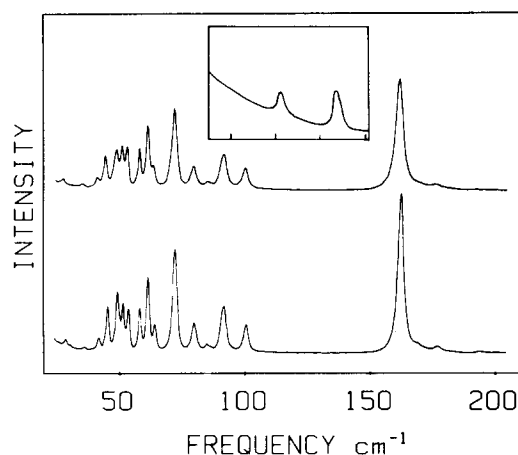
TABLE II. Raman and infrared spectra of $ZnBr_2$ peak frequencies in cm^{-1}.[a]

Raman		
$T = 300$ K	$T = 125$ K	Group
27	27	(w)
34.5	35.5	(w)
40.5	41	A
44	45	B
48	48.5	B
50	51	(m)
52.5	53	B
57	57.5	A
60.5	60.5	A
63	63.5	C
71	71.5	B
79	79	A
84.5	84.5	C
91	91	A
99.5	100	(m)
161	162	(m)
–	~168(sh)	(w)
175	175.5	(w)
192.5	193	(w)
~198	199	(w)

Infrared	
$T = 300$ K	$T = 90$ K
53	54
64	66
74	76
90	92
~117(sh)	~123(sh)
~165(sh)	~171(sh)
196	200
226	229

[a] (sh): Shoulder. (w): Weak (no polarization analysis possible). (m): Probably multiplet peak, showing no polarization properties characteristic of any group. A,B,C: Group label. See Fig. 3 for polarization properties.

tions) rather than any fundamental change in crystal structure.

Far infrared spectra of powder samples at 300 and 90 K are shown in Fig. 4. Peak frequencies are listed on the right-

FIG. 4. Far infrared spectra of $ZnBr_2$, at $T = 300$ K (upper curve) and at $T = 90$ K (lower curve). Inset is far infrared spectrum of $NiBr_2$ at $T = 110$ K for the same frequency range $40-260$ cm^{-1} from Ref. 13. Resolution: 2.5 cm^{-1}.

hand side of Table II. In contrast to the sharp well-resolved Raman spectra, the infrared spectra display the usual characteristics of strongly absorbing powders: scattering losses at high frequencies and broad peaks resulting from frequency dependence on the variable sample thickness together with reflection losses. In addition, for this hygroscopic sample, because of the large surface area of the powder, contamination by water is possible, although there is no direct evidence for this. Because of these difficulties, more weight will be given to the Raman data in the discussion which follows.

The results of the x-ray diffraction study of $ZnBr_2$ indicate a tetragonal structure with $a = 11.389(4)$ Å, $c = 21.773(9)$ Å, space group $I4_1/acd$, and $Z = 32$ (16 formula units per primitive cell). While the crystallographic results are given in detail elsewhere,[7] it is useful to note several features of the crystal structure here, particularly since it relates to the analysis of the vibrational spectra in the next section. The structure consists of an approximately cubic close packed array of Br atoms with Zn filling 1/4 of the tetrahedral sites. The major feature of the structure is the "supertetrahedral" cage-like unit, Zn_4Br_{10}, as shown in Fig. 5. Each Zn atom is tetrahedrally coordinated to 4 Br atoms, and the Zn–Br–Zn connections between the supertetrahedra are nonlinear.
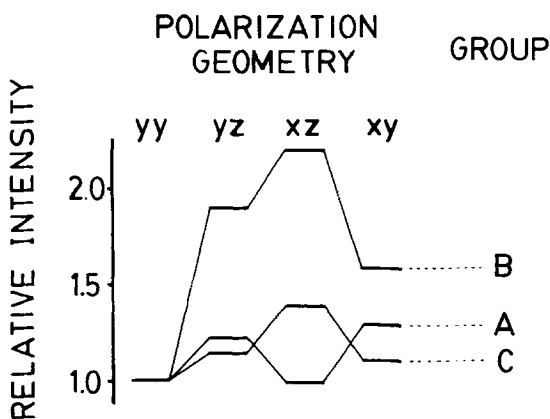

POLARIZATION GEOMETRY   GROUP

FIG. 3. Polarization effects of Raman peaks. Relative intensities of typical peaks in each of three groups A, B, and C. Incident laser beam is along z; scattered light along x; crystal orientation unknown. Intensities have been ratioed against those for the yy configuration in which the electric vectors of both the incident and scattered beams are perpendicular to the xz plane.
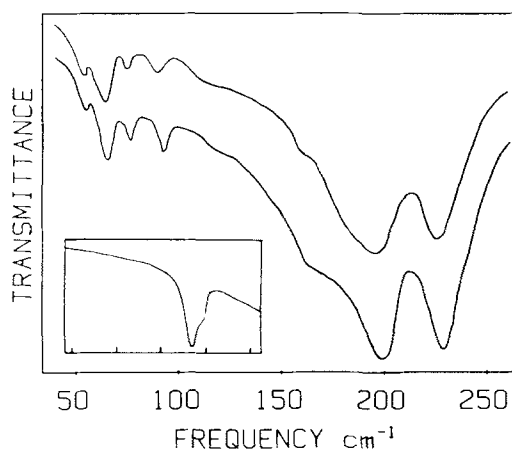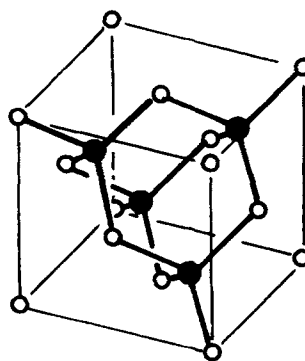

FIG. 5. The supertetrahedral Zn_4Br_{10} subunit of the crystal structure of $ZnBr_2$. Bromine atoms: open circles; zinc atoms: filled circles.

DISCUSSION

As indicated in the Introduction, the heat capacity results for $ZnBr_2$ were undertaken in order to provide a guide to the lattice heat capacity of $NiBr_2$, so that an analysis of the magnetic contribution to the heat capacity of that salt could be made. On the basis of their similar molecular weights and the absence of magnetic contributions in $ZnBr_2$, one would have "expected" the heat capacity of $ZnBr_2$ to be less than that of $NiBr_2$ if the two compounds were isostructural as reported.[5,6] However, a comparison of C_P for the two compounds, as illustrated in Fig. 1, shows that for the region from $T \sim 10$ K to $T \sim 100$ K, the opposite is observed. In fact, in the region from $T = 20$ K to $T = 30$ K, C_p of $ZnBr_2$ exceeds that of $NiBr_2$ by about a factor of 2. This rather surprising result was the first indication that $ZnBr_2$ and $NiBr_2$ are not isomorphous.

The Raman spectra of $ZnBr_2$ clearly support this conclusion in that the contrast between the simple two peak Raman spectra observed for crystals of the $CdCl_2$ and CdI_2 structures,[12,13] and those shown in Fig. 2 for $ZnBr_2$ could hardly be greater. Although the infrared spectrum is somewhat less definitive, it is clear that it also has many more peaks than the two predicted and observed for these simpler structures.[12,13] The rich vibrational spectra of $ZnBr_2$ are immediately indicative of a large unit cell. The number of noncoincidences between Raman and infrared peak frequencies also supports a centrosymmetric structure for this crystal. The fact that many of these vibrations have low frequencies qualitatively explains the anomalously large heat capacity values at low temperatures.

The strongest Raman peak $(\sim 162\ cm^{-1})$ is in the vicinity of the symmetric stretch (ν_1) for $ZnBr_4^{2-}$ ions, observed in aqueous solutions,[14] and the strong doublet in the far infrared spectrum $(200, 229\ cm^{-1})$ similarly corresponds to the asymmetric stretch (ν_3) of these tetrahedral units. In addition, the frequency positions of the other two fundamentals of $ZnBr_4^{2-}$ $(\nu_2 \sim 65\ cm^{-1}; \nu_4 \sim 86\ cm^{-1})$ are close to where peaks are observed in both Raman and infrared spectra in the present work. Of course, the actual normal mode frequency distribution for such a large unit cell will be very complicated, but the spectra are generally compatible with the structural interpretation that the building blocks of the $ZnBr_2$ crystal are indeed $ZnBr_4^{2-}$ tetrahedral units.[7]

A somewhat more quantitative interpretation is possible by using the group theoretical correlation method.[15] This relates the degrees of freedom of all ions in the unit cell to their symmetry species at their sites and those pertaining to the whole unit cell, as illustrated in Fig. 6 (left-hand side). In the space group $I4_1/acd$ (D_{4h}^{20}), the 16 Zn^{2+} ions and 16 of the Br^- ions are on general sites, while the other 16 Br^- ions occupy two sets of C_2 sites. The net result is that 44 Raman and 26 infrared peaks are predicted for $ZnBr_2$. (The larger number of Raman peaks is a consequence of the fact that of the 10 unit cell representations, 4 are Raman active, 4 are inactive, and only 2 are infrared active.) The numbers of components are larger than the actual peaks observed (20 Raman, 8 infrared) by a factor of over 2.

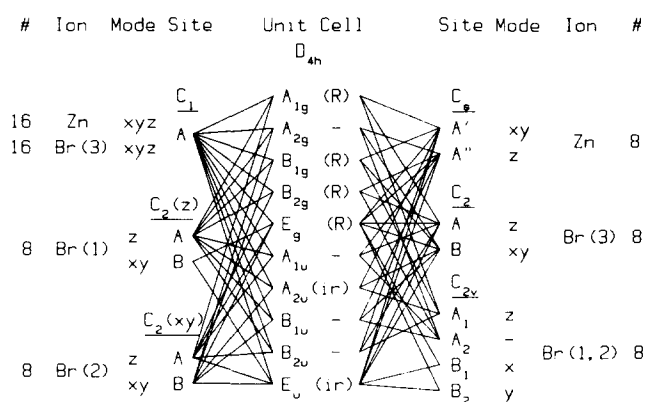It would appear that the actual structure of $ZnBr_2$ is a distortion of a somewhat more symmetrical structure with a

FIG. 6. Correlation diagrams for $ZnBr_2$. R: Raman active; ir: infrared active. Left: true structure, space group $D_{4h}^{20}(I4_1/acd)$. Right: approximate structure, space group $D_{4h}^{15}(P4_2/nmc)$.

primitive unit cell of half the size (eight formula units per primitive cell). In other words, the normal mode frequencies depend mainly on short range interactions and are insensitive to the form of coupling with other more distant ions. This results in some modes being effectively degenerate, and a reduction in the number of peaks observed. Some indirect supportive evidence for this is provided by the polarization studies. Some quite strong peaks did not fall into any particular groups, perhaps because they contained unresolved components of different symmetries.

Of the various possibilities leading to a smaller unit cell, based on the classification of space groups by geometric units,[16] the one described by space group $P4_2/nmc$ (D_{4h}^{15}) is favored. This space group retains the Zn_4Br_{10} supertetrahedral group and the bent Zn–Br–Zn connections between supertetrahedra. Relative to the true space group, the unit cell is reduced by a factor of 2 in the c direction, and by a further factor of $\sqrt{2}$ in the a and b directions (half the diagonals of the original unit cell). Eight Br^- ions are on C_{2v} sites, the other eight are on C_2 sites and the Zn^{2+} ions are on C_s sites. The net result, as shown by the correlation diagram in Fig. 6 (right-hand side), is the prediction of 23 Raman and 14 infrared peaks, much closer to the actual numbers observed.

It should be noted that in any large unit cell, there will be some modes in which neighboring ions move as a block in phase with each other but against similar blocks. (A similar interpretation has been given to explain the Raman spectrum of the molecular crystal hydrogen sulfide, which has 16 molecules in the unit cell.[17]) The large effective mass of these vibrations will lead to very low frequency modes, which will contribute greatly to the low temperature heat capacity.

The results of the Raman and infrared experiments have been used to calculate the heat capacity of $ZnBr_2$ as a function of temperature, as described below.

In the absence of a complete spectroscopic assignment, a simplified calculation[18] of the optical contribution to the heat capacity has been made:

$$C_v(\text{optic}) = \frac{3R}{q}\frac{[3(q-1)]}{44+26}\left\{\frac{44}{m}\sum_{i=1}^{m}\phi_E(x_i)\right.$$
$$\left. + \frac{26}{n}\sum_{j=1}^{n}\phi_E(x_j)\right\},$$

where

$$\phi_E(x_i) = \frac{x_i^2\, e^{x_i}}{(e^{x_i} - 1)^2}$$

and

$$x_i = \frac{h\omega_i}{2\pi kT},$$

h is Planck's constant, ω_i is the frequency of the ith mode, k is Boltzmann's constant, T is the temperature, q is the number of atoms per primitive unit cell (= 3 atoms/molecule × 16 molecules/primitive cell here), m(= 20) is the number of Raman modes included in the calculation, and n(= 8) is the number of infrared modes included. The acoustic contribution to the heat capacity of $ZnBr_2$ has been assessed from that of $NiBr_2$, such that:

$$C_v(\text{acoustic, } ZnBr_2) = C_v(\text{acoustic, } NiBr_2)/16,$$

where

$$C_v(\text{acoustic, } NiBr_2) = C_v(\text{lattice, } NiBr_2)$$
$$- C_v(\text{optic, } NiBr_2),$$

and the lattice and optic heat capacities of $NiBr_2$ are taken from Ref. 4 and a calculation based on the $NiBr_2$ Raman spectrum, respectively. Although the sum of the optical and acoustic contributions to the heat capacity for $ZnBr_2$ is the molar heat capacity at constant volume C_v, we are unable to assess $C_p - C_v$ for $ZnBr_2$ due to the absence of thermal expansion data. However, we can say for inorganic solids that C_p is nearly equal to C_v.

A comparison of the calculated and experimental values of C_p is shown in Fig. 7. The two are in very good agreement, especially in the low temperature region where the experimental values are so much greater than those of $NiBr_2$ (Fig. 1). As one might expect, the calculated and experimental heat capacity values are also in good agreement at higher temperatures, where C_v approaches $9R$ (= 74.8 J K^{-1} mol^{-1}). However, the calculated heat capacity is higher than the measured values at intermediate temperatures ($\sim 15\%$ too high at $T = 50$ K), and this difference is most likely attributable to giving equal weight to each of the observed Raman and infrared frequencies in the calculation of the optical contribution to C_v. The fact that the calculated heat capacity is higher than the measured in this temperature range, and yet the two agree well at lower temperatures,
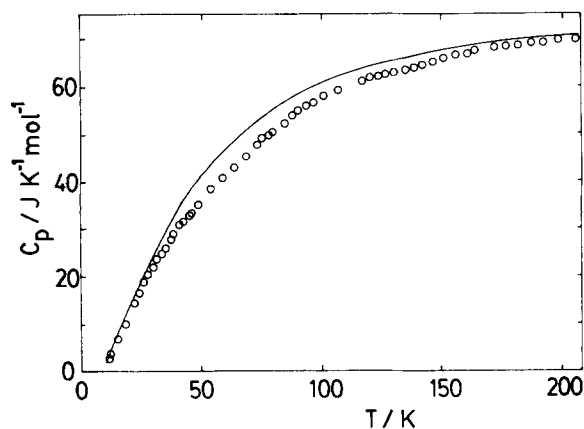

FIG. 7. Comparison of the calculated (full line) and experimental (open circles) heat capacity of $ZnBr_2$ as a function of temperature.

indicates that modes with frequencies between ~ 70 and ~ 100 cm^{-1} should be weighted slightly less than the other modes.

CONCLUDING REMARKS

The results of these combined calorimetric, spectroscopic, and x-ray diffraction investigations of anhydrous zinc bromide are all consistent with its crystal structure being much more complex than that of MX_2 compounds with the $CdCl_2$ type of layered arrangement. The unit cell of $ZnBr_2$ is large ($Z = 32$), and the space group is body centered tetragonal ($I\,4_1/acd$). A group theoretical analysis based on this structure indicates that there should be 44 Raman and 26 infrared active modes, approximately twice the numbers observed. The difference has been attributed to near-degeneracies that can arise in a large unit cell, in which certain modes differ from others only in the phase relationships between ions quite distant from and therefore weakly coupled to each other. An additional effect in a large cell is that neighboring ions can move together as a block against similar blocks. The large effective mass for these modes leads to rather low vibrational frequencies, which accounts for the unusually high heat capacity at low temperatures in $ZnBr_2$. A calculation of the heat capacity based on a simplified weighting of the Raman and infrared frequencies leads to a much improved agreement with the observed values, especially at low temperatures.

ACKNOWLEDGMENTS

[1] P. Day, A. Dinsdale, E. R. Krausz, and D. J. Robbins, J. Phys. C **9**, 2481 (1976).
[2] A. Adam, D. Billerey, C. Terrier, R. Mainard, L. P. Regnault, J. Rossat-Mignod, and P. Mériel, Solid State Commun. **35**, 1 (1980).
[3] E. Rastelli, A. Tassi, and L. Reatto, Physica B **97**, 1 (1979).
[4] M. A. White and L. A. K. Staveley, J. Phys. C **15**, L169 (1982).
[5] R. W. G. Wyckoff, *Crystal Structures*, 2nd ed. (Interscience, New York, 1963), Vol. 1.
[6] See, for example, P. J. Durant and B. Durant, *Introduction to Advanced Inorganic Chemistry*, 2nd ed. (Longman, London, 1970).
[7] C. Chieh and M. A. White, Z. Kristallogr. (in press, 1983).
[8] C. G. Waterfield and L. A. K. Staveley, Trans. Faraday Soc. **63**, 2349 (1967).
[9] E. F. Westrum, Jr. (personal communication, 1981).
[10] W. M. Sears and J. A. Morrison, J. Phys. Chem. Solids **40**, 503 (1979).
[11] D. Durand, L. C. Scavarda do Carmo, A. Anderson, and F. Lüty, Phys. Rev. B **22**, 4005 (1980).
[12] A. Anderson, Y. W. Lo, and J. P. Todoeschuck, Spectrosc. Lett. **14**, 105 (1981).
[13] A. Anderson and Y. W. Lo, Spectrosc. Lett. **14**, 603 (1981).
[14] H. Kanno and J. Hiraishi, J. Raman Spectrosc. **9**, 85 (1980).
[15] W. G. Fateley, F. R. Dollish, N. T. McDevitt, and F. F. Bentley, *Infrared and Raman Selection Rules for Molecular and Lattice Vibrations* (Wiley-Interscience, New York, 1972).
[16] C. Chieh, Acta Crystallogr. Sect. A **39**, 415 (1983).
[17] A. Anderson, O. S. Binbrek, and H. C. Tang, J. Raman Spectrosc. **6**, 213 (1977).
[18] R. A. Smith, *Wave Mechanics of Crystalline Solids* (Chapman and Hall, London, 1969).